A simulation study using GEANT4 and EpiXS to examine radiation properties for multilayer shielding materials used in nuclear reactor environments

MD MINHAZUL MOSTAFA, A. S. MOLLAH
Department of Nuclear Science and Engineering
Military Institute of Science and Technology (MIST)
Mirpur-1216, Dhaka
BANGLADESH

Abstract: - In a nuclear reactor, gamma rays are produced primarily by nuclear fission and neutron capture on an atomic nucleus. Although fission produces considerable radioactivity, a number of barriers are used to maintain the radiation dose at a safe level. For the (n, γ) reaction, the neutrons penetrate the RPVs and other structural shielding materials producing further gamma rays. The application of multiple shielding layers increases attenuation and consequently reduces dose rates in confined spaces. This study investigates the interactions between gamma rays and diverse shielding materials through comprehensive simulations and analyses to assess their efficacy in attenuating radiation. Geant4, a powerful tool for particle simulation, plays a pivotal role in predicting and optimizing the shielding properties of these materials. The findings contribute valuable insights to the field of radiation protection, offering advancements in the design and application of nuclear shielding materials across a range of contexts and industries. The methodology involves the development of a Geant4-based simulation model that accurately represents the experimental setup. This model incorporates details of the gamma-ray radiation source, shielding materials, and the surrounding environment. Monte Carlo simulations are performed to track the trajectory of gamma rays, allowing for the determination of radiation dose rates at specified locations and aiming to enhance reactor safety and radiation protection measures as per IAEA guidelines and regulatory dose limits.

Key-Words: - Geant4, Reactor Pressure Vessel (RPVs), VVER, IAEA, EpiXS, Half-Value Layer (HVL).

Received: April 29, 2025. Revised: August 14, 2025. Accepted: October 8, 2025. Published: November 19, 2025.

1 Introduction

Gamma (γ) is a high-penetrating radiation energy that is generated from nuclear reactions in a nuclear reactor. Neutron-induced reactions (n, γ) produce huge amounts of heat energy as a form of gamma radiation in the nuclear reactor. This gamma radiation is harmful to living beings as well as the environment. To mitigate gamma radiation from the core of the reactor to the exclusion zone, multi-layer shielding materials are used [1].

Zirconium alloy is known as Zircaloy and is used as a cladding material for fuel rods in nuclear reactors. Zircaloy offers a range of mechanical benefits due to its diverse properties, including superior hardness, ductility, and corrosion resistance. Zirconium, the primary refractory metal in Zircaloy, demonstrates exceptional resistance to corrosion, a low thermal neutron absorption cross-section, and high heat tolerance [2].

Water (H_2O) is used in a nuclear reactor, which acts as both a coolant and a moderator. In nuclear reactors, water serves as a moderator to decrease the speed of neutrons generated by fission reactions. Water has a high moderating ratio and acts as a good neutron moderator but a poor neutron absorber [3].

Another layer is used in the Reactor Pressure Vessels (RPVs), which are made of ferritic steel. RPVs a thick steel container that holds nuclear fuel and other key reactor components in a nuclear power plant. It is capable of high-pressure, temperature cyclic loading, and neutron irradiation during reactor operation. RPVs provide one of the several barriers that keep radioactive material out of the environment [4][5].

The reinforced concrete containment structure serves as the ultimate barrier, separating nuclear reactors and the environment from any potential nuclear accidents. Concrete plays a crucial role in nuclear power plants, offering a sturdy shield against radiation. Recently, blended concrete composed of composite materials has been utilized as radiation shielding concrete (RSC) [6][7].

A recent study showed that individual materials investigated the effectiveness of gamma-shielding properties of cladding materials, moderators, RPVs materials, and composite concrete. To date, research on individual materials has predominantly concentrated on their interaction with high-energy neutrons. Consequently, the gamma attenuation capabilities of multi-layer shielding materials remain largely unexplored, particularly within thermal energy ranges, as this data has not yet been documented in the literature [1].

This study investigates the gamma radiation shielding abilities of multi-layer shielding materials. The shielding properties of cladding materials, moderators, RPVs materials, and composite concrete were compared to each other. Using the Monte Carlo simulation toolkit Geant4, the gamma attenuation coefficients of these materials are theoretically analyzed across a wide energy spectrum ranging from 0.1 to 20 MeV [8].

2 Materials

Four different materials were used in this study. Each material density is different from the others. Nuclear fuel cladding material, Zircaloy-4, is used in this study and is highly corrosion-resistant and has a low absorption cross-section. The second shielding material is light water(H_2O), acting as a moderator and coolant. The third shielding layer material is thick steel, which is ferritic steel. It is used for its rich mechanical properties and shielding effectiveness. The final shielding material, known as RSC (SWX-261 Neutron Putty), is a composite concrete material. It comprises concrete infused with 10% boron and possesses three times the hydrogen content of standard concrete [3][9][10].

Table 1. Composition of Zircaloy-4 (Weight Percentage) [9]

Name	Zircaloy-4
UNS Grade	R60804
Tin	1.20-1.70
Iron	0.18-0.24
Chromium	0.07-0.13
Oxygen	Per P.O.
Iron + Chromium	0.23-0.37

Table 2. Light Water (H_2O) composition [3]

Name	Density (g/cm^3)	Mass% H_2 content	H-atoms/cm^3	Gamm Shielding
Water	1.0	11	6.7x10’22	Poor

Table 3. Chemical Composition of VVER-1200 RPVs (Weight Percentage) [4][5]

Material Name	C	Cr	Ni	Mo	V
15Cr2NiMoVA steel	0.14%	2.6%	0.31%	0.79%	0.63%

Table 4. Chemical Composition of Concrete [10]

Trade Name	H-atom density/ cm^3	Hydrogen weight percent	Boron atom density/ cm^3	Boron natural isotope distribution	Boron weight percent	Total Density
SWX-261 Neutron Putty	5.91×10^{22}	8.95 %	6.16×10^{21}	19.6 % ^{10}B and 80.4 % ^{11}B	10.0 %	1.11 g / cm^3 (69 lbs. / ft^3)

3 Theory

A key component of any material's shielding capabilities, the mass attenuation coefficient is correlated with the material's density, gamma energy, and Z_{eff}. The inverse proportion of the attenuation coefficient is known as HVL. It stands for the thickness of a substance needed to cut the initial gamma radiation energy in half. The total atomic number of the composite material during gamma radiation interactions is represented by the effective atomic number (Z_{eff}). The average number of electrons per unit mass is known as the effective electron density (N_{eff}), and it determines how gamma rays interact with a material. Beer-Lambert's law states that the gamma radiation intensity will be attenuated as shown in Equation (1) [11][12][13].

$$I = I_o e^{-\mu(E)t} \quad (1)$$

where $\mu(E)$ (cm^{-1}) is the material's linear attenuation factor at the specific energy, and I_0 and I are the unattenuated and attenuated gamma ray beam intensities. The linear thickness of the absorber sample is denoted by t (cm). The gamma mass attenuation coefficient (μ_m) is determined using Equation (2) [11][12][13].

$$I = I_o e^{-(\mu/\rho)t_d} = I_o e^{-\mu_m t_d} \quad (2)$$

where μ (cm^{-1}) is the linear attenuation coefficient, $\mu_m = \mu/\rho$ (cm^2/g) is the mass attenuation coefficient, t_d (g/cm^2) is the density thickness of the absorber sample, and I_0 and I are the unattenuated and attenuated gamma ray beam intensities.

The relationship between t and t_d can be established by Equation (3) [11][12][13].

$$t_d = \rho \times t \quad (3)$$

The following Equation (4) provides the relationship between μ and μ_m [11][12][13].

$$\mu = \mu_m \times \rho \quad (4)$$

A buildup factor B is added to Equation (5) as a correction factor to account for scattered beams when a broad beam geometry is used [1][14].

$$I = BI_o e^{-\mu(E)t} \quad (5)$$

In a multilayer shield, the radiation intensities that emerge from the layers that follow are influenced by the layers that come before them. Equation (6) can be used to calculate the resulting intensity I_3. Nevertheless, it would appear that changing the order of the materials would have no impact, given the commutative property of multiplication in equation (6) [1][14].

$$I_3 = I_o B_1 B_2 B_3 \, e^{-\{\mu_1(E)t_1 + \mu_2(E)t_2 + \mu_3(E)t_3\}} \quad (6)$$

The mixture rule determines the total mass attenuation coefficient, or $(\mu/\rho)_{compound\ or\ mixture}$, for any chemical compound or elemental mixture, as shown in Equation (7) [11][12][13].

$$(\mu/\rho)_{compound} = \sum_i (\mu/\rho)_i w_i \quad (7)$$

where w_i and $(\mu/\rho)_i$ represent the ith constituent element's mass attenuation coefficient and weight fraction, respectively. The fraction by weight (w_i) of a chemical compound is determined by,

$w_i = \frac{n_i A_i}{\sum_i n_i A_i}$, where n_i is the number of formula units and A_i is the ith element's atomic weight and $\sum_i w_i = 1$.

The total linear attenuation coefficient, $\mu_{compound\ or\ mixture}$ of the compound or mixture, can then be simply found by multiplying the total mass attenuation coefficient, $(\mu/\rho)_{compound}$, by its density ρ, as specified in Equation (8) [11][12][13].

$$\mu_{compound} = \left(\frac{\mu}{\rho}\right)_{compound} \times \rho \quad (8)$$

Half Value Layer (HVL) is the thickness of a shield or an absorber that reduces the radiation level by a factor of 2, that is to half the initial level and is calculated by the following Equation (9) [11][12][13].

$$HVL = \frac{\ln(2)}{\mu} = \frac{0.693}{\mu} \quad (9)$$

The total molecular cross-section can be found using Equation (10) [11][12][13].

$$\sigma_{t,m} = \left(\frac{\mu}{\rho}\right)\frac{A_t}{N_A} = \frac{1}{N_A}\left(\frac{\mu}{\rho}\right)_C \sum_i n_i A_i \quad (10)$$

Moreover, the total atomic cross-section can be calculated by Equation (11) [11][12][13].

$$\sigma_{t,a} = \sigma_{t,m} \frac{1}{\sum_i^n (n_i)} = \frac{\sigma_{t,m}}{\sum n_i} \quad (11)$$

where (N_A) is Avogadro's number, ($A_t = \Sigma n_i A_i$) is the molecular weight, (A_i) is the atomic weight of an element of the compound, and (n_i) is the total number of atoms. While the total electronic cross-section for the element is given by Equation (12) [11][12][13].

$$\sigma_{t,el} = \frac{1}{N_A} \sum_i^n \frac{f_i A_i}{Z_i} (\mu_m)_i = \frac{1}{N_A} \sum_i f_i \frac{A_i}{Z_i} \left(\frac{\mu}{\rho}\right)_i \quad (12)$$

where (f_i) is the number of atoms of element (i) relative to the total number of atoms of all elements in the compound, and (Zi) is the atomic number of the ith element in the compound. The effective atomic number ($Zeff$) of the compound could be found from the ratio between the total atomic cross-section and the total electronic cross-section given by Equation (13) [11][12][13].

$$Z_{eff} = \frac{\sigma_{t,a}}{\sigma_{t,el}} \quad (13)$$

While the effective electron density is given by Equation (14) [11][12][13].

$$N_{eff} = \frac{\mu_m}{\sigma_{t,el}} = \frac{\left(\frac{\mu}{\rho}\right)_C}{\sigma_{t,el}} = \frac{N_A n_{tot} Z_{eff}}{\sum_i n_i A_i} \quad (14)$$

where; $\left(\frac{\mu}{\rho}\right)_C$ is the compound's mass attenuation coefficient and $\sigma_{t,el}$ is the total electronic cross section.

4 Methodology

Geant4 is a Monte Carlo simulation tool widely used for studying radiation properties. In this study, the energy range of gamma was between 0.1 MeV to 20 MeV. Here, a fixed monoenergetic source is used, with an energy range from 0.1 MeV to 20 MeV. For multi-layer shielding, 4 materials are used in this study. In this study, we investigate the mass attenuation, HVL, effective atomic density, and electron density. Later, the outcome result is compared with EpiXS, which is a Windows-based radiation software for photon attenuation, dosimetry, and shielding based on the EPICS2017 and EPDL9 databases that can obtain the photon cross-section data for any sample. Also, for the graph, matplotlib is used [15][16][17].

To ensure quantitative accuracy, the simulation results obtained from GEANT4 were systematically validated against EpiXS reference data for identical material compositions and photon energies. The comparison involved evaluating the mass attenuation coefficient (μ/ρ), half-value layer (HVL), effective atomic number (Z_{eff}), and effective electron density (N_{eff}) across the entire 0.1–20 MeV energy range. The percentage deviation between both datasets was calculated and consistently found to be below 0.07%. This high level of agreement confirms the precision of the GEANT4 model and its suitability for predicting photon attenuation behavior in multilayer reactor shielding systems.

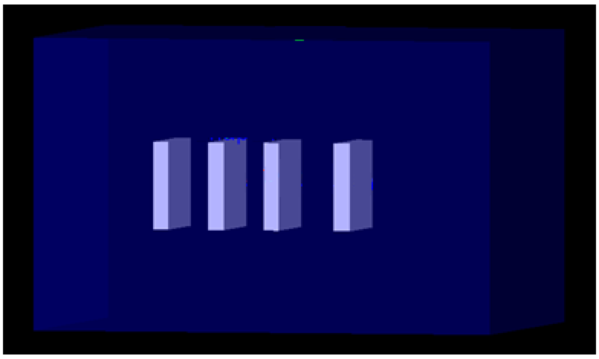

Figure 1. Visualization before running the Geant4 simulation Of 4 shielding materials.

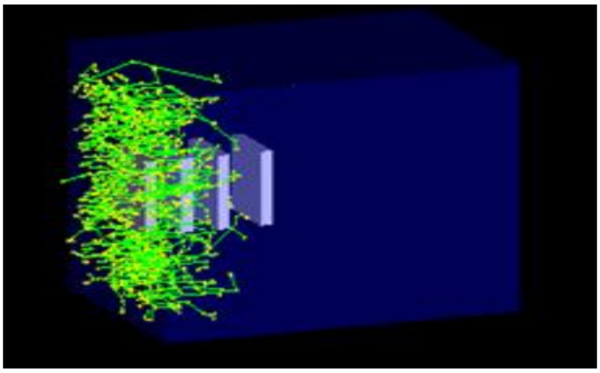

Figure 2. Visualization after running the Geant4 simulation

5 Result

The simulation results for μ/ρ, HVL, Z_{eff}, and N_{eff} show excellent agreement with EpiXS data, with deviations typically below 0.07%. Mass Attenuation Coefficient decreases with increasing photon energy, reflecting the transition from photoelectric dominance at low energies to Compton scattering and then pair production. HVL increases with energy, indicating reduced attenuation efficiency at higher photon energies. Z_{eff} and N_{eff} remain stable across the energy range, with small variations corresponding to changes in interaction mechanisms. Matplotlib software is used to plot the graphs of mass attenuation coefficient, HVL, effective atomic number (Z_{eff}), and effective electron density (N_{eff}) in the studied energy range [18][19].

$$\Delta\% = \left(\frac{EpiXS\ Result - Geant4\ Result}{EpiXS\ Result}\right) \times 100 \quad (15)$$

5.1 Gamma-Shielding Properties and Validation of Geant4 Code Results

Table 5. Displays the results and percentage changes in the mass attenuation coefficients using Geant4 and EpiXS.

Gamma Energy (MeV)	Mass Attenuation Coefficient µm (cm2/g)		
	EpiXS	Geant4	%Δ
0.1	0.950636	0.950083	0.058171582
0.15	0.374938	0.374709	0.061076765
0.2	0.221994	0.221867	0.057208753
0.25	0.161612	0.161681	-0.042694849
0.3	0.13133	0.1313001	0.022767075
0.35	0.113452	0.113384	0.059937242
0.4	0.101693	0.101624	0.067851278
0.45	0.0932374	0.0931996	0.040541671
0.5	0.0868946	0.0868481	0.053513107
0.55	0.0817206	0.0816804	0.049192003
0.6	0.0775736	0.0775391	0.044473893
0.65	0.0739535	0.0739061	0.06409433
0.7	0.0708607	0.0708272	0.047275852
0.75	0.0681492	0.0681024	0.068672853
0.8	0.0657342	0.0657003	0.051571328
0.85	0.0635487	0.0635108	0.0596393
0.9	0.061586	0.0615463	0.064462703
0.95	0.0598053	0.059781	0.04063185
1	0.0581441	0.0581249	0.033021407
2	0.0414573	0.0414371	0.048724833
3	0.0363596	0.0363367	0.062981991
4	0.0343536	0.0343318	0.063457687
5	0.0336127	0.0336008	0.035403285
6	0.033469	0.0334486	0.060951926
7	0.0336625	0.0336476	0.044262904
8	0.0340573	0.0340346	0.066652377
9	0.0345518	0.0345371	0.042544817
10	0.0351089	0.0350876	0.060668378
11	0.0356887	0.0356673	0.059962957
12	0.0362876	0.0362641	0.064760414
13	0.0368713	0.0368505	0.05641244
14	0.037432	0.037413	0.050758709
15	0.0379898	0.0379634	0.069492337
16	0.0385375	0.0385149	0.058644178
17	0.0390357	0.0390163	0.049698097
18	0.0395812	0.0395607	0.051792265
19	0.0400617	0.0400481	0.033947636
20	0.0405716	0.0405591	0.030809729

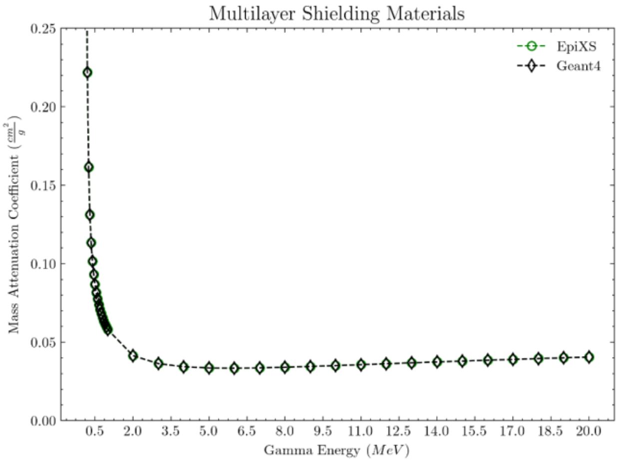

Figure 3. The mass attenuation coefficients using Geant4 and EpiXS

Table 6. Displays the results and percentage changes in the HVLs using Geant4 and EpiXS.

Gamma Energy (MeV)	Half-value layers (HVL)		
	EpiXS	Geant4	%Δ
0.1	0.0772395	0.0772073	0.041688514
0.15	0.195837	0.1957548	0.041973682
0.2	0.33076	0.33083	-0.021163381
0.25	0.45434	0.454271	0.015186864
0.3	0.5591	0.55897	0.023251654
0.35	0.647203	0.647072	0.020240944
0.4	0.722042	0.721834	0.028807189
0.45	0.787523	0.787251	0.034538674
0.5	0.845008	0.844807	0.023786757
0.55	0.898508	0.898291	0.024151148
0.6	0.946542	0.946343	0.021023895
0.65	0.992876	0.992616	0.026186553
0.7	1.03621	1.035903	0.029627199
0.75	1.07744	1.07704	0.037125037
0.8	1.11702	1.11673	0.025961934
0.85	1.15544	1.15501	0.03721526
0.9	1.19226	1.191931	0.027594652
0.95	1.22776	1.22747	0.023620252
1	1.26284	1.26246	0.030090906
2	1.77114	1.77037	0.043474824
3	2.01946	2.01872	0.036643459
4	2.13738	2.13643	0.04444694
5	2.18449	2.18394	0.025177501
6	2.19387	2.19261	0.057432756
7	2.18126	2.18007	0.054555624
8	2.15597	2.15473	0.057514715
9	2.12512	2.12406	0.049879536

10	2.0914	2.0908	0.028688917
11	2.05742	2.05643	0.048118517
12	2.02346	2.02273	0.036076819
13	1.99143	1.99051	0.046197958
14	1.9616	1.96073	0.04435155
15	1.9328	1.9318	0.051738411
16	1.90533	1.90443	0.047235912
17	1.88101	1.88006	0.050504782
18	1.85509	1.85437	0.038812133
19	1.83284	1.83243	0.022369656
20	1.8098	1.80934	0.025417173

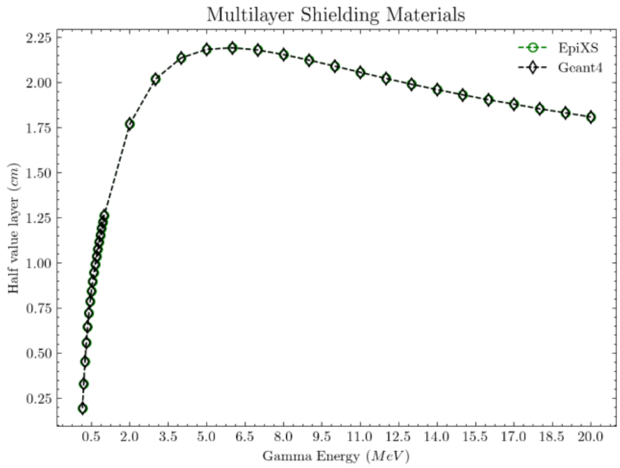

Figure 4. The HVLs using Geant4 and EpiXS.

Table 7. Displays the results and percentage changes in the effective atomic number *(*Z_{eff}*)* using Geant4 and EpiXS.

Gamma Energy (MeV)	Effective atomic numbers (Z_{eff})		
	EpiXS	Geant4	%Δ
0.1	39.368931	39.353742	0.038581185
0.15	38.498812	38.484389	0.037463494
0.2	37.684719	37.670642	0.037354664
0.25	37.076081	37.060764	0.041312349
0.3	36.655668	36.640597	0.04111506
0.35	36.370597	36.350437	0.05542939
0.4	36.171954	36.163348	0.023791913
0.45	36.03296	36.023488	0.026287044
0.5	35.932347	35.920564	0.03279218
0.55	35.854206	35.840761	0.037499087
0.6	35.79855	35.775454	0.06451658
0.65	35.751084	35.743764	0.020474904
0.7	35.714563	35.694345	0.05660996
0.75	35.68477	35.673445	0.031736228
0.8	35.660357	35.635564	0.069525384
0.85	35.640739	35.627954	0.035871871
0.9	35.623941	35.607654	0.045719254
0.95	35.609349	35.594385	0.042022672
1	35.597264	35.581676	0.043789882
2	35.674234	35.663433	0.030276754
3	35.994832	35.974864	0.05547463
4	36.325067	36.310343	0.040533993
5	36.618672	36.607634	0.030143092
6	36.867452	36.854754	0.034442304
7	37.079462	37.064078	0.041489275
8	37.257517	37.240076	0.04681203
9	37.409448	37.3944204	0.040170601
10	37.539752	37.523476	0.043356706
11	37.651914	37.640476	0.03037827
12	37.748391	37.730752	0.046727819
13	37.831917	37.816047	0.041948707
14	37.905104	37.887892	0.045408133
15	37.968872	37.952046	0.044315249
16	38.02552	38.01762	0.020775521
17	38.075696	38.060671	0.039460868
18	38.121326	38.110746	0.027753494
19	38.16191	38.147642	0.037388066
20	38.199483	38.185076	0.03771517

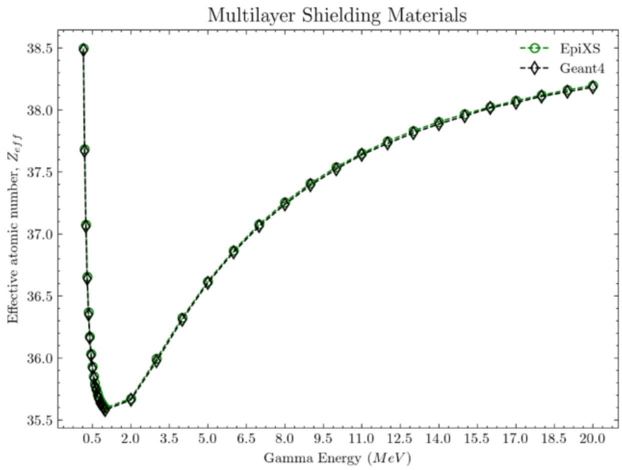

Figure 5. Displays effective atomic numbers (Z_{eff}) using Geant4 and EpiXS.

Table 8. Shows the outcomes and percentage variations of effective electron density (N_{eff}) utilizing Geant4 and EpiXS.

Gamma Energy (MeV)	Effective electron densities (N_{eff})		
	EpiXS	Geant4	%Δ
0.1	2.942943	2.941467	0.050153877
0.15	2.8779	2.87634	0.054206192
0.2	2.817044	2.81607	0.03457525
0.25	2.771546	2.770174	0.049503057
0.3	2.740119	2.738752	0.049888344
0.35	2.718809	2.718075	0.026997115
0.4	2.70396	2.702431	0.056546694
0.45	2.69357	2.69412	-0.020418998
0.5	2.686049	2.685043	0.037452779
0.55	2.680207	2.679043	0.043429481
0.6	2.676047	2.675044	0.037480657
0.65	2.672499	2.671573	0.034649218
0.7	2.669769	2.668537	0.046146315
0.75	2.667542	2.666074	0.055031936
0.8	2.665717	2.664061	0.062122123

0.85	2.66425	2.66306	0.044665478
0.9	2.662994	2.662175	0.030754857
0.95	2.661904	2.660734	0.043953501
1	2.661	2.65972	0.048102217
2	2.666754	2.665863	0.033411406
3	2.69072	2.69011	0.022670512
4	2.715406	2.714053	0.049826803
5	2.737353	2.736075	0.046687439
6	2.755951	2.755013	0.034035438
7	2.771799	2.7711048	0.025045106
8	2.785109	2.785001	0.003877766
9	2.796466	2.795073	0.049812871
10	2.806207	2.805046	0.041372572
11	2.814591	2.813476	0.039614992
12	2.821803	2.820104	0.060209731
13	2.828047	2.827046	0.035395451
14	2.833518	2.832043	0.052055431
15	2.838285	2.837034	0.044075912
16	2.84252	2.841234	0.045241546
17	2.84627	2.845043	0.043109051
18	2.849681	2.848043	0.057480118
19	2.852715	2.851063	0.057909746
20	2.855524	2.854076	0.050708732

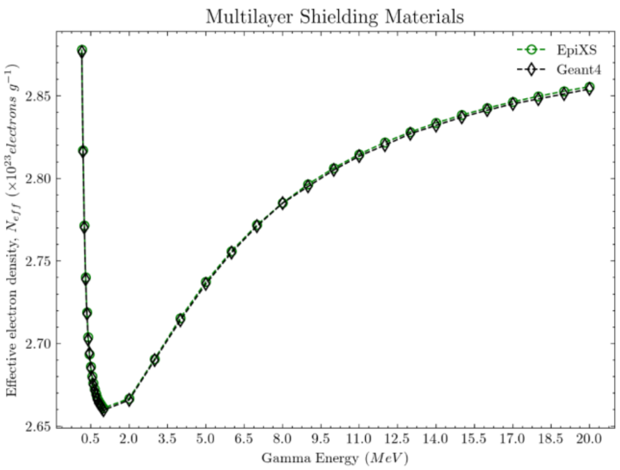

Figure 6. The effective electron densities (N_{eff}) using Geant4 and EpiXS.

6 Discussion

The comparative analysis between Geant4 simulation results and EpiXS reference data reveals a remarkably close agreement, with percent deviations generally below 0.07% for all evaluated parameters. This level of accuracy underscores the reliability of the Geant4 Monte Carlo toolkit for modeling photon attenuation through complex multilayer shielding arrangements in nuclear reactor environments.

Mass Attenuation Coefficient (μ/ρ) values exhibit a decreasing trend as photon energy increases from 0.1 MeV to approximately 2 MeV. This behavior is attributed to the shift in dominant photon interaction mechanisms. At low energies, the photoelectric effect dominates, where photon absorption probability scales approximately with Z^4 –Z^5 , leading to strong attenuation in high-Z materials. As photon energy increases, Compton scattering becomes the prevailing process, characterized by quasi-elastic collisions between photons and bound electrons, resulting in reduced attenuation efficiency. Beyond ~2 MeV, pair production begins to contribute as photons acquire sufficient energy to create electron–positron pairs, causing the attenuation curve to gradually flatten. These transitions collectively explain the smooth, physically consistent variation of μ/ρ and HVL observed in the simulated results.

Half-Value Layer (HVL) values increase with energy, reflecting the reduced effectiveness of shielding at higher photon energies. This highlights the importance of increasing shield thickness or using higher-Z materials to maintain protection levels against high-energy photons. The close match between simulation and EpiXS HVL values confirms the model's accuracy in predicting practical shielding requirements.

The near constancy of Z_{eff} and N_{eff} across the photon energy spectrum indicates that the multilayer system maintains compositional stability, with variations primarily reflecting transitions in dominant interaction mechanisms rather than material response inconsistencies. These parameters are primarily determined by the elemental composition of the shielding materials and are less sensitive to photon energy. However, small variations observed correspond to shifts in dominant interaction mechanisms, especially around the transition energies between photoelectric and Compton scattering dominance.

Overall, the results validate the design concept of graded multilayer shielding, where each layer is optimized for different interaction regimes:

- Zircaloy-4 cladding for structural integrity and low neutron absorption.
- Water moderator for neutron moderation with secondary photon shielding.
- Ferritic steel RPV for intermediate-energy photon attenuation.

- Borated composite concrete for final-stage gamma and neutron attenuation.

This combination provides effective protection across a broad gamma energy spectrum while complying with IAEA occupational and public dose limits.

7 Conclusion

This study demonstrated the successful application of the Geant4 Monte Carlo simulation toolkit in the modeling of photon attenuation in a multilayered shielding system characteristic of VVER-1200 nuclear reactors. The key findings are:

- High accuracy: Simulated μ/ρ, HVL, Z_{eff}, and N_{eff} are in good agreement with EpiXS reference data, with discrepancies below 0.07%.
- Physical consistency: Trends observed in attenuation parameters are physically consistent with expectations from photon-matter interaction physics.
- Shielding performance: The selected multilayer configuration adequately attenuates gamma photons across the 0.1–20 MeV range, confirming its feasibility in nuclear reactor radiation shielding.
- Design validation: Results confirm the continued use of graded material designs to optimize the shielding performance for different photon energy ranges.

Future work must be extended to neutron attenuation in mixed radiation fields and examine the effects of thermal-hydraulic conditions on shielding effectiveness. Such extensions would increase the overall knowledge of in-reactor shielding performance and safety margins. The strong agreement between GEANT4 and EpiXS data, together with the physically consistent attenuation trends, provides confidence in the model's capability for future reactor shielding and safety studies.

Acknowledgement:

The authors would like to extend their thanks to the Department of Nuclear Science and Engineering at the Military Institute of Science and Technology (MIST), Dhaka, Bangladesh, for providing the necessary laboratory support for this research. The authors would also like to thank **Ariful Islam** for providing support with relevant concepts.

References:

[1] M. Arif Sazali, N. K. Alang Md Rashid, and K. Hamzah, A review on multilayer radiation shielding, *IOP Conf. Ser.: Mater. Sci. Eng.*, vol. 555, no. 1, p. 012008, June 2019, doi: 10.1088/1757-899X/555/1/012008.

[2] C. L. Whitmarsh, *Review of Zircaloy-2 and Zircaloy-4 Properties Relevant to N.S. Savannah Reactor Design*. Oak Ridge National Laboratory for the U.S. Atomic Energy Commission, 1962.

[3] D. R. McAlister, Neutron Shielding Materials, 2018.

[4] D. Kovács and D. Kemény, Investigation of VVER-1200 reactor pressure vessel's material, *IOP Conf. Ser.: Mater. Sci. Eng.*, vol. 903, no. 1, p. 012051, Aug. 2020, doi: 10.1088/1757-899X/903/1/012051.

[5] J. Brynda, V. Cerny, and R. Konop, VVER reactor pressure vessel materials database and monitoring of ageing and lifetime evaluation, 2002.

[6] Ali M. Onaizi, Mugahed Amran, Waiching Tang, Nour Betoush, Mohammad Alhassan, Raizal S.M. Rashid, Mohammad Fares Yasin, K.H. Bayagoob, Sagheer A. Onaizi, Radiation-shielding concrete: A review of materials, performance, and the impact of radiation on concrete properties, Journal of Building Engineering, Volume 97, 2024, 110800, ISSN 2352-7102, https://doi.org/10.1016/j.jobe.2024.110800.

[7] A. N. Perevoshchikova, I. V. Valtsifer, N. B. Kondrashova, and N. S. Voronina, The physical and mechanical properties of concrete with multifunctional additive, *Nanotekhnologii v Stroitel'stve*, vol. 16, no. 2, pp. 170–179, 2024.

[8] H. Akhdar, M. W. Marashdeh, and M. AlAqeel, Investigation of gamma radiation shielding properties of polyethylene glycol in the energy range from 8.67 to 23.19 keV, *Nuclear Engineering and Technology*, vol. 54, no. 2, pp. 701–708, 2022.

[9] Zircaloy-4(Alloy Zr4) (UNS R60804), AZoM. Accessed: Aug. 26, 2025. [Online]. Available: https://www.azom.com/article.aspx?ArticleID=7644

[10] Neutron & Gamma Putties | Shieldwerx. Accessed: Aug. 26, 2025. [Online]. Available:

https://www.shieldwerx.com/neutron-gamma-putties

[11] T. Saniye and K. Adnan, Measurement of Total Electronic Cross-Section, Total Atomic Cross-Section, Effective Atomic Numbers, Effective Electron Densities and Kerma for Some Br Compounds, *Journal ISSN*, vol. 2766, p. 2276, 2021.

[12] Md Minhazul Mostafa and A. S. Mollah, Evaluating Radiation Characteristics of Cr-Coated Silicon Carbide and Zircaloy Claddings in a PWR Fuel Assembly: A Simulation Study Employing GEANT4 and EpiXS, International Journal of Chemical Engineering and Materials, vol. 4, pp. 19-28, 2025.

[13] R. Biswas, H. Sahadath, A. S. Mollah, and M. F. Huq, Calculation of gamma-ray attenuation parameters for locally developed shielding material: Polyboron, *Journal of Radiation Research and Applied Sciences*, vol. 9, no. 1, pp. 26–34, 2016.

[14] A. A. Alfuraih, Simulation of gamma-ray transmission buildup factors for stratified spherical layers, *Dose-Response*, vol. 20, no. 1, p. 15593258211068625, 2022.

[15] N. MacFadden, S. Peggs, and C. Gulliford, Development and validation of a Geant4 radiation shielding simulation framework, Brookhaven National Lab.(BNL), Upton, NY (United States), 2018.

[16] A. Cilliers *et al.*, Geant4 in a new role-Reactor Physics

[17] S. Cao, Y. Zeng, S. Yang, and S. Cao, Research on Python data visualization technology, in *Journal of physics: Conference series*, IOP Publishing, 2021, p. 012122.

[18] H. Akhdar and M. Alshehri, Geant4 simulation of photon-and neutron-shielding capabilities of biopolymer blends of poly (lactic acid) and poly (hydroxybutyrate), *Polymers*, vol. 15, no. 21, p. 4257, 2023.

[19] H. Akhdar and R. Alotaibi, Geant4 simulation of the effect of different composites on polyimide photon and neutron shielding properties, *Polymers*, vol. 15, no. 8, p. 1973, 2023.

Contribution of Individual Authors to the Creation of a Scientific Article (Ghostwriting Policy)

Md Minhazul Mostafa led the study's conception, modeling design, data analysis, manuscript drafting, literature review, resource provision, and writing. A. S. Mollah provided conceptual input, review, editing, interpretation of results, and supervision. All authors have reviewed the findings and approved the final manuscript version.

Please visit Contributor Roles Taxonomy (CRediT) that contains several roles:
www.wseas.org/multimedia/contributor-role-instruction.pdf

Sources of Funding for Research Presented in a Scientific Article or Scientific Article Itself
This research received no external funding.

Data Availability Statement
The data presented in this research are accessible upon request to the corresponding author.

Conflict of Interest
The authors report no conflicts of interest related to this work.